Metamagnetic crossover in the quasikagome Ising Kondo-lattice compound CeIrSn

S. Tsuda,[1] C. L. Yang,[1] Y. Shimura,[1] K. Umeo,[2] H. Fukuoka,[3] Y. Yamane,[1] T. Onimaru,[1] T. Takabatake,[1] N. Kikugawa,[4] T. Terashima,[4] H. T. Hirose,[4] S. Uji,[4] S. Kittaka,[5] and T. Sakakibara[5]

[1]*Department of Quantum matter, AdSM, Hiroshima University, Higashi-Hiroshima 739-8530, Japan*

[2]*Cryogenics and Instrumental Analysis Division, N-BARD, Hiroshima University, Higashi-Hiroshima 739-8526, Japan*

[3]*Department of Applied Chemistry, Graduate School of Engineering, Hiroshima University, Higashi-Hiroshima 739-8527, Japan*

[4]*National Institute for Materials Science, Tsukuba, Ibaraki 305-0003, Japan*

[5]*Institute for Solid State Physics, University of Tokyo, Kashiwa, Chiba 277-8581, Japan*

(Received 22 June 2018; published 29 October 2018)

The Ce atoms in CeIrSn form a quasikagome lattice in the hexagonal c plane. Our single-crystal x-ray diffraction analysis has confirmed the absence of superstructure in the ZrNiAl-type structure. Motivated by the recent observation of quantum critical behaviors in the isostructural and isoelectronic compound CeRhSn, we have studied low-temperature properties of single-crystalline samples of CeIrSn by measuring the electrical resistivity, magnetic susceptibility χ, magnetization M, and specific heat C down to 0.05 K. Our study does not show evidence of a long-range magnetic ordering down to the lowest temperature. The $\chi(T)$ data show an Ising character, $\chi_c \gg \chi_a$, and power-law behaviors at low temperatures: $\chi_c \propto T^{-0.8}$ and $\chi_a \propto T^{-0.6}$. When external field B is applied along the a axis, both $M(B)$ and $C(B)/T$ exhibit metamagnetic anomalies at 5.5 T, which resemble those observed in CeRhSn at 3.5 T. We attribute the metamagnetic crossover under in-plane magnetic fields to the alleviation of magnetic frustration inherent in the quasikagome Ising Kondo lattice.

DOI: 10.1103/PhysRevB.98.155147

I. INTRODUCTION

Kondo lattice systems with geometrically frustrated arrangements of Ce and Yb atoms have attracted much attention because the frustration induces unusual quantum critical behaviors at low temperatures [1–4]. The local $4f$ electrons of Ce and Yb ions are coupled to conduction electrons, leading to the onsite Kondo effect which screens the local moment. This effect competes with the intersite Ruderman-Kittel-Kasuya-Yosida (RKKY) interaction. The ratio K between the Kondo temperature T_K and the RKKY interaction was used to be the decisive parameter to determine the ground state of conventional Kondo lattice systems. In geometrically frustrated Kondo systems such as kagome and Shastry-Sutherland lattices [5–11], however, another tuning parameter Q has been introduced to describe the strength of quantum fluctuations induced by the frustration among magnetic moments [9–11]. A kagome Kondo lattice with antiferromagnetic (AFM) nearest-neighbor interaction is expected to have unconventional quantum critical points (QCPs) depending on the degrees of K and Q. However, it is often difficult to locate a specific compound in the proposed phase diagram drawn by the two parameters K and Q. It is mainly because Q in metallic Kondo systems cannot be quantified by the ratio between the paramagnetic Curie temperature and magnetic ordering temperature, unlike in insulating frustrated systems with local moments [12]. Therefore, experimental studies of a series of kagome Kondo lattice systems are highly requested to understand the effect of geometrical frustration on the QC behaviors.

A notable frustrated Kondo lattice is CePdAl in which Ce atoms form a quasikagome lattice in the hexagonal ZrNiAl-type structure with the space group $P\bar{6}2m$, which lacks inversion symmetry [13]. The local moments of nearly trivalent Ce ions have an Ising character along the hexagonal c axis. Within a single quasikagome layer, only two thirds of moments participate in the long-range AFM order at $T_N = 2.7$ K, while the other one third of moments remain paramagnetic due to the frustration effect [5,14]. Application of hydrostatic pressure suppresses T_N and brings the system close to a QCP at 0.95 GPa [15].

An isostructural compound CeRhSn has a rather high $T_K \sim 240$ K [16,17] and therefore exhibits no magnetic order down to 0.05 K [18]. The specific heat divided by temperature, C/T, has a plateau at 0.2 J/K^2 mol and turns up on cooling below 0.2 K [19]. At a constant temperature below 0.2 K, C/T as a function of $B \parallel a$ exhibits a peak at 3.5 T [19], which field value coincides with that of the peak in the ac magnetic susceptibility at 0.03 K [20]. These anomalies induced by $B \parallel a$ were considered to be the results of release of the magnetic frustration by the field applied perpendicular to the Ising axis. Furthermore, the thermal expansion coefficient along the a axis divided by temperature, α_a/T, diverges on cooling below 0.3 K, which is thought to be caused by the magnetic frustration remaining in the ground state [19]. Recently, an additional evidence for the magnetic frustrations in CeRhSn has been given by the magnetostriction measurement under uniaxial stress [21]. In fact, the quantum criticality has disappeared under uniaxial stress applied along the a direction. When the quasikagome lattice is distorted by the stress of 60 MPa, a complex magnetic phase diagram arises for $B \parallel a$. In addition, a magnetic order in zero field has been induced by the substitution of Pd for Rh at a low level of 10% [20]. All the experimental facts corroborate that CeRhSn is located very close to the QCP related to magnetic frustration.

CeIrSn is isostructural and isoelectronic with CeRhSn in which the lattice parameters are very close to each other within 0.3% [22]. Previous structural refinement on a single crystal taken from an arc-melted sample has indicated that the Ir atom in the Ir-Sn plane, Ir2, has very large anisotropic displacement parameters [23]. In fact, the U_{33} parameter describing the vibration along the c axis is twice as large as U_{11} for Ir2 and U_{33} for the Ir1 in the Ir-Ce plane. This large displacement parameter of U_{33} for Ir2 hints to formation of a superstructure as observed for ZrIrSn, in which the c-axis parameter is doubled [24]. If the doubling were not perfect in the crystal of CeIrSn, structural disorder or local stress should affect the ground state properties. In the present work, we have carefully examined the possible superstructure formation in the single crystal prepared by the Czochralski method.

Physical properties of CeIrSn have been so far reported only for the polycrystalline samples in the temperature range above 1.4 K. The magnetic susceptibility $\chi(T)$ shows a hump at around 170 K [25]. The thermopower S and the magnetic part of the electrical resistivity, $\rho_m = \rho(\mathrm{CeIrSn}) - \rho(\mathrm{LaIrSn})$, exhibit a broad maximum at around 300 and 100 K, respectively [26]. These properties are characteristics of Ce compounds in the valence-fluctuating regime. The T_K is estimated as 480 K from the relation of $T_\mathrm{K} = 1.6T_\mathrm{sm}$, where T_sm denotes the temperature at the maximum of $S(T)$ [27]. Note that the value of T_K for CeIrSn is twice higher than that for CeRhSn. Because of the stronger Kondo coupling in CeIrSn, this system is assumed to be positioned far away from the QCP in the proposed phase diagram for the frustrated Kondo lattice. However, we should recall that frustration-induced quantum critical behaviors in CeRhSn manifest themselves at temperatures only below 1 K. Furthermore, these behaviors are suppressed by the application of magnetic field or uniaxial stress along the hexagonal a axis [19,21]. Therefore, it is worth investigating whether or not similar quantum critical behaviors appear in CeIrSn at low temperatures and in applied magnetic fields. We report here on the magnetic, transport, and specific-heat measurements on the single-crystalline samples of CeIrSn at temperatures down to 0.05 K and in magnetic fields up to 17.5 T.

II. EXPERIMENTS

Single-crystalline samples of CeIrSn have been grown by the Czochralski method from a stoichiometric melt of 25 g in a tungsten crucible in an RF induction furnace filled with purified argon gas, as described previously [17]. The compositions of both ends of the single crystals of 50 mm in length were examined by electron-beam microanalysis (EPMA). Neither impurity phase nor deviation in the stoichiometry was detected within the 1% resolution.

For x-ray diffraction experiments, we isolated a tiny single crystal with a size of $0.02 \times 0.05 \times 0.13$ mm via mechanical fragmentation of the as grown crystal. X-ray diffraction intensity data were collected with a Bruker Smart Apex II CCD diffractometer with graphite monochromated MoKα radiation, $\lambda = 0.071073$ nm. To reduce the error due to thermal vibrations, the crystal was cooled to 123 K in the cold stream of an open-flow nitrogen cryostat. The structure was solved by direct methods and refined with the Bruker SHELX-2016 package [28,29].

For the transport, magnetic, and specific-heat measurements, the single crystals were oriented along the a and c axes by the back-reflection Laue x-ray pattern. The oriented crystals were cut into appropriate dimensions for each measurement by a spark erosion technique. The measurements of $\rho(T)$ and $S(T)$ were performed with a standard four-terminal method and a seesaw heating method [30], respectively. An adiabatic demagnetization refrigerator mF-ADR50 was used to measure $\rho(T)$ down to 0.04 K in magnetic fields up to 6 T. For the measurements of dc magnetization, we used a Quantum Design MPMS in the temperature range from 1.8 to 300 K and a homemade capacitive Faraday force magnetometer in a ^{3}He cryostat down to 0.4 K under magnetic fields applied along the a and c directions. The temperature- and magnetic-field dependences of χ_{ac} were measured under $B_{ac} = 372$ μT at the frequency of 67.2 Hz in a ^{3}He-^{4}He dilution refrigerator equipped with a 20 T magnet at Tsukuba Magnet Laboratory, NIMS. Using this magnet system, the field dependences of ρ in both longitudinal and transverse configurations were measured by the ac method. The temperature dependence of $C(T)$ from 0.4 to 20 K was measured by the relaxation method in a Quantum Design PPMS. For lower temperatures down to 0.07 K, $C(T)$ was measured in constant magnetic fields up to 8 T by an integration method [31] and the field dependence $C(B)$ at constant temperatures was measured by a relaxation method with a ^{3}He-^{4}He dilution refrigerator at the Institute for Solid State Physics, University of Tokyo.

III. RESULTS AND DISCUSSION

The results of the refinement of crystal structure of CeIrSn are summarized in Tables I and II. Our analysis on the x-ray diffraction data obtained at 123 K is consistent with the previous one for the data taken at room temperature [23]. Because of the lower temperature in our experiment, the obtained anisotropic displacement parameters are approximately half of the reported data. The magnitude of U_{33} for Ir2 is 40% larger than U_{11} and U_{22}, which is similar to that found at room temperature [23]. This large value of U_{33} was attributed to the consequence of the intermediate valence character of the Ce ions [23]. We carefully examined the presence of any superstructure by checking diffraction images. Nevertheless, no superspots were observed in the images, thus we conclude that CeIrSn has no superstructure.

Figure 1 shows the temperature dependences of $\rho(T)$ and $S(T)$ for the single crystal of CeIrSn together with the data for CeRhSn derived from Refs. [17,32]. The large anisotropy $\rho_a(T) > \rho_c(T)$ is common for both compounds, while the temperature at the maximum of $\rho_a(T)$ is twice higher in CeIrSn than in CeRhSn. The temperature at the maximum in $S(T)$, T_sm, for CeIrSn is also twice higher than that for CeRhSn, while the anisotropy in $S(T)$ is rather stronger for CeIrSn. If T_K is taken as 1.6 times of T_sm [27], then T_K is estimated to be 480 and 240 K for CeIrSn and CeRhSn, respectively. It is noteworthy that only $S_a(T)$ for CeIrSn exhibits a negative minimum at around 14 K, suggesting the presence of an energy scale much lower than T_K.

TABLE I. Crystallographic data and structural refinement parameters of CeIrSn at 123 K.

Composition from EPMA	CeIrSn
Single crystal dimensions (μm)	$20 \times 50 \times 130$
Temperature (K)	123
Radiation, λ (nm)	Mo Kα, 0.071073
Crystal system	Hexagonal
Space group	$P\bar{6}2m$ (No. 189)
Number of formula units in unit cell: Z	3
Unit cell dimensions (nm)	
a	0.74279(9)
c	0.40674(5)
Cell volume (nm^3)	0.19435(5)
Calculated density (g/cm^3)	11.561
Absorption coefficient μ_{abs} (mm^{-1})	77.66
Range in hkl	$\pm 8, \pm 8, \pm 4$
θ range	3° to 25°
Number of total reflections	1673
Number of independent reflections	147 ($R_{int} = 4.19\%$)
Number of refined parameters	15
R_{all}	0.0107
$wR2$	0.0258
Goodness-of-fit on F^2	1.132
Extinction coefficient	0.0094(8)

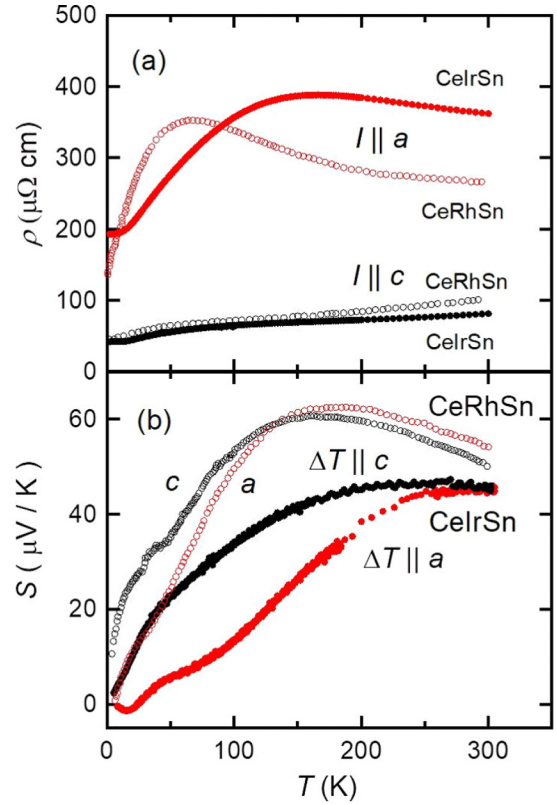

FIG. 1. Temperature dependences of the electrical resistivity ρ and thermopower S for single crystals of CeIrSn and CeRhSn along the hexagonal a and c axes. The data for CeRhSn are derived from Refs. [17,32].

The low-temperature data of $\rho(T)$ down to 0.04 K in various constant magnetic fields B up to 6 T are shown in Fig. 2. At first glance, there is no kinklike anomaly expected for a long-range magnetic transition. Zero-field μSR experiments also indicate the absence of magnetic transition [33]. In zero field at $T < 0.5$ K, $\rho_a(T)$ and $\rho_c(T)$ follow the form $\rho(T) = \rho_0 + AT^n$ with $n = 1.0$ and 1.5, respectively, whose values are smaller than 2.0 expected for a Fermi liquid ground state. We applied magnetic field B in parallel to the direction of the electrical current I to avoid the effect of cyclotron motions of charge carriers. With increasing B to 6 T, n approaches 2.0, indicating the recovery of a Fermi liquid state. Thereby, the magnitude of $\rho_a(T)$ decreases steadily with B in the whole temperature range below 5 K, while $\rho_c(T)$ shows complex variations with B at $T < 1$ K. The data of field dependence of $\rho(B)$ will be presented and discussed afterward.

Figure 3 shows a double logarithmic plot of dc susceptibility $\chi(T)$ for CeIrSn in a field of 0.1 T applied parallel to the a and c axes, respectively. Thereby, the data for CeRhSn are represented for comparison [17]. It is noteworthy that the Curie-Weiss fit to data of $1/\chi_c(T)$ for $T > 250$ K yields the paramagnetic Curie temperature $\boldsymbol{\Theta}_P$ of -724 and -394 K for CeIrSn and CeRhSn, respectively. If we take the half of $|\boldsymbol{\Theta}_P|$ as T_K [34], then the values of T_K of 362 and 197 K are comparable with those estimated from the maximum temperature of $S(T)$. The Ising nature of the Ce moments in the quasikagome lattice is manifested in the large anisotropy $\chi_c(T) \gg \chi_a(T)$. With decreasing temperature below 7 K, the magnitudes of $\chi_c(T)$ and $\chi_a(T)$ for CeIrSn exceed those of CeRhSn, respectively. Below 1.0 K, $\chi_c(T)$ and $\chi_a(T)$ for CeIrSn follow the power law $\chi(T) \propto T^{-n}$ with $n = 0.8$ and 0.6, respectively, and the values are comparable with 0.8 and 0.35 for CeRhSn [17]. The divergent behavior in both $\chi_c(T)$ and $\chi_a(T)$ seems to render the two compounds outside the Fermi liquid regime.

Let us compare the specific heat data of CeIrSn with those of CeRhSn derived from Refs. [17,19]. As is shown in the inset of Fig. 4, C/T data of both compounds decrease in

TABLE II. Atomic coordinates and anisotropic displacement parameters (pm^2) for CeIrSn at 123 K. U_{eq} is defined as one third of the trace of the orthogonalized U_{ij} tensor. The anisotropic displacement factor exponent takes the form: $-2\pi^2[(ha^*)^2U_{11} + \cdots + 2hka^*b^*U_{12}]$. $U_{13} = U_{23} = 0$.

Atom	Site	x/a	y/b	z/c	U_{11}	U_{22}	U_{33}	U_{12}	U_{eq}
Ce	3f	0	0.41340(17)	0	28(6)	23(5)	31(5)	14(3)	27(3)
Ir1	1a	0	0	0	26(4)	U_{11}	9(6)	13(2)	21(3)
Ir2	2d	2/3	1/3	1/2	36(3)	U_{11}	50(5)	18(2)	41(3)
Sn	3g	0.74829(16)	0	1/2	23(5)	28(7)	25(6)	14(3)	25(3)

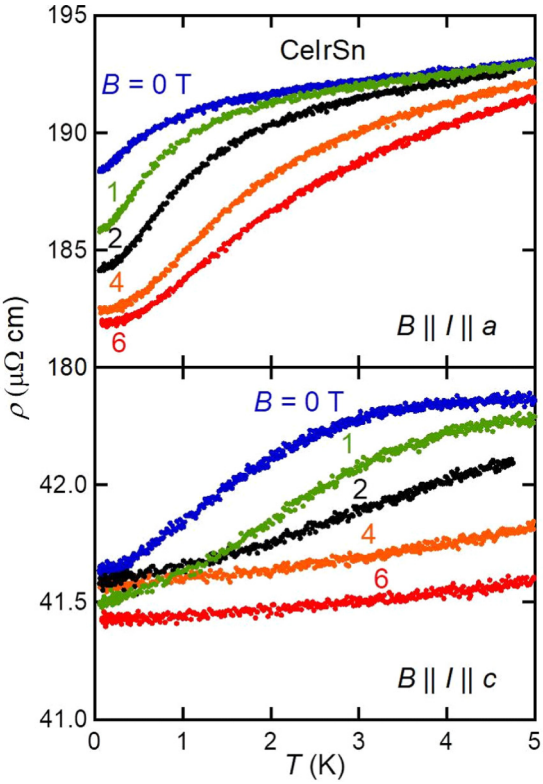

FIG. 2. Temperature dependence of the electrical resistivity ρ for the single crystal of CeIrSn down to 0.04 K in various constant magnetic fields up to 6 T in the longitudinal configurations $B \parallel I \parallel a$ and $B \parallel I \parallel c$.

proportion to T^2 on cooling to 7 K and turn up on further cooling. The double logarithmic plot of C/T vs T is presented in Fig. 4. The value of C/T for CeRhSn has a plateau at around 1.0–0.4 K, whereas that for CeIrSn continuously increases. After the C/T curve for CeIrSn exceeds that for CeRhSn, it increases as T^{-3} down to 0.07 K, the lowest temperature of our measurements. The T^{-3} dependence retains

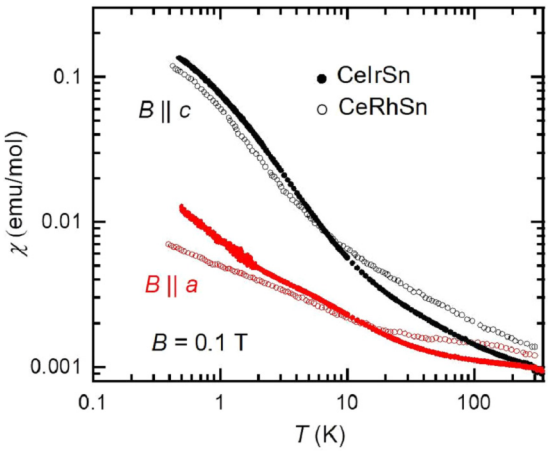

FIG. 3. The dc magnetic susceptibility of single crystals of CeIrSn and CeRhSn measured in an external field $B = 0.1$ T applied parallel to the hexagonal a and c axes, respectively. The data for CeRhSn are derived from Ref. [17].

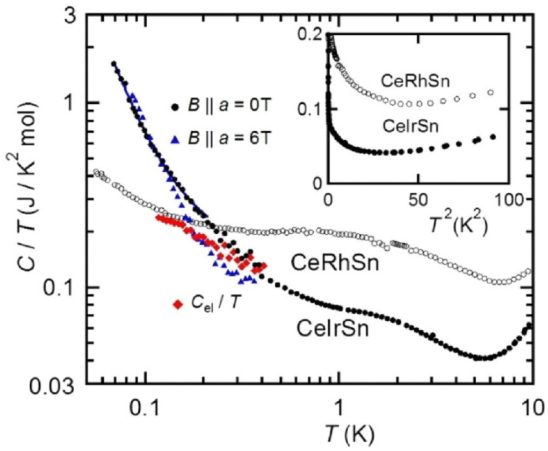

FIG. 4. Double logarithmic plot of the specific heat divided by temperature C/T vs T for single crystals of CeIrSn and CeRhSn. The data for CeRhSn are derived from Refs. [17,19]. The triangles denote the data in an external field $B \parallel a = 6$ T. The solid line represents the fit to the zero-field data including the nuclear contribution, and the diamonds denote the electronic contribution (see text). The inset shows the plot of C/T vs T^2 for CeIrSn and CeRhSn.

even in an external field $B \parallel a = 6$ T at $T < 0.1$ K as shown by triangles in Fig. 4, while the values in $B \parallel a$ are suppressed at $T > 0.15$ K. The robust T^{-3} dependence of C/T against magnetic field is the signature of the Schottky-type specific heat arising from the interaction of nuclear quadrupoles with electric field gradient [35]. In the present system, ^{191}Ir and ^{193}Ir nuclei have spins of 3/2 and thus quadrupole moments, while ^{103}Rh nuclei with spins of 1/2 have no quadrupole moment in CeRhSn. Because the site symmetry for both sites of Ir1 and Ir2 contains the symmetry element $\bar{6}$, there is an electric field gradient which interacts with the nuclear quadrupole moments and thus splits the energy level. The data in zero field were tentatively fitted by the form, $C/T = \alpha/T^3 - \beta\, lnT + \gamma$, assuming that the phonon contribution is negligible compared with other terms at $T < 2$ K. The solid line in Fig. 4 shows the fit with parameters: $\alpha = 0.000457$ JK/mol, $\beta = 0.153$ J/K^2 mol, and $\gamma = 0.087$ J/K^2 mol. The electronic part, $C_{el}/T = C/T - \alpha/T^3$, is represented by diamond marks. We measured $C(T)$ under several fixed magnetic fields $B \parallel a$ up to 8 T, but the errors in the data did not allow us to find any sharp anomaly in the temperature scan. Therefore, we have measured the field dependence $C(B \parallel a)$ at fixed temperatures 0.25 K and 0.5 K, where the nuclear contribution is largely suppressed. The data of C/T are plotted as a function of $B \parallel a$ in Fig. 5(c). The field dependence at 0.25 K shows a definite peak at 5.5 T, which becomes broader on heating to 0.5 K. This field induced anomaly in C/T will be discussed in the next paragraph combined with the metamagnetic anomaly in the magnetization.

Here, we recall that a metamagnetic crossover in CeRhSn occurs in the magnetization process $M(B)$ and $C(B)/T$ under the field of 3.5 T applied in-plane of the quasikagome lattice [19,20]. This crossover was considered as a result of reorientation of the moments in the quasikagome Kondo lattice [19]. Expecting similar metamagnetic anomaly in CeIrSn,

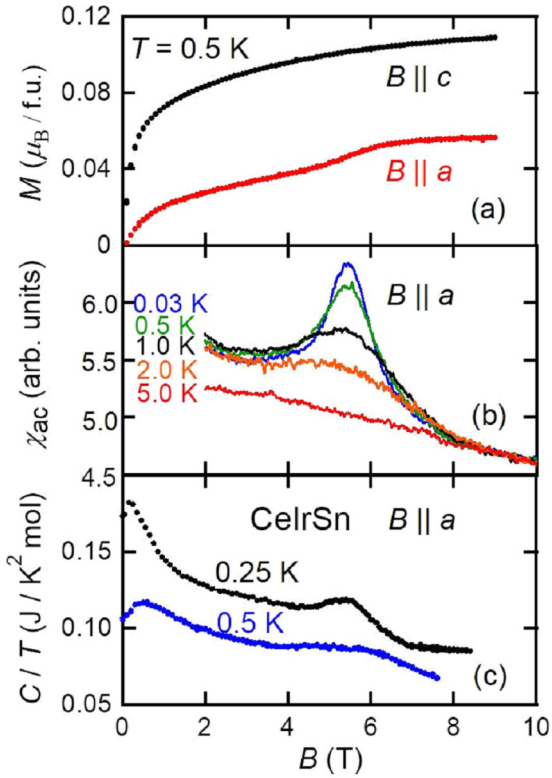

FIG. 5. (a) Magnetization curves $M(B)$ in $B \parallel a$ and $B \parallel c$ at $T = 0.5$ K for the single crystal of CeIrSn. (b) The ac susceptibility as a function of $B \parallel a$ at different temperatures. The data were vertically shifted to be converged at $B = 10$ T. (c) The dependence of the specific heat divided by temperature C/T on the external field $B \parallel a$ at $T = 0.25$ and 0.5 K.

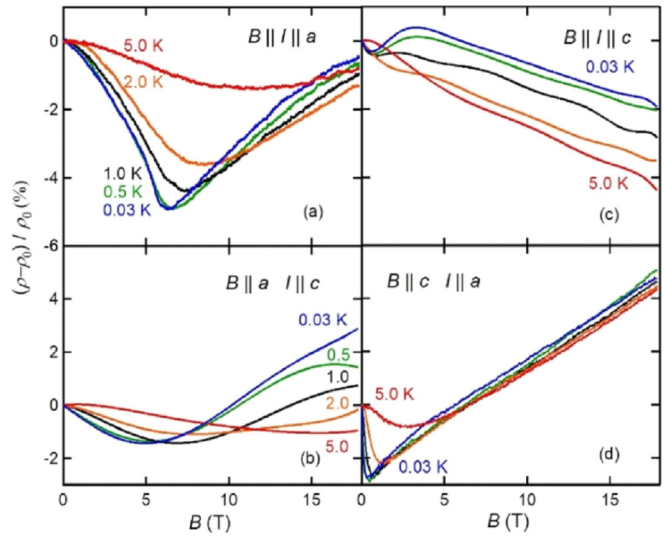

FIG. 6. Normalized magnetoresistance of the single crystal of CeIrSn at different temperatures for the longitudinal configuration [(a) $B \parallel I \parallel a$ and (c) $B \parallel I \parallel c$] and transverse configuration [(b) $B \parallel a$ and $I \parallel c$ and (d) $B \parallel c$ and $I \parallel a$].

we have measured the isothermal magnetization $M(B)$ at 0.5 K, which is the lowest accessible temperature for our magnetization measurements. As shown in Fig. 5(a), $M(B \parallel a)$ does exhibit a metamagnetic increase at 5.5 T. On the other hand, $M(B \parallel c)$ initially rises to approximately 0.08 μ_B/f.u. and slowly increases to 0.11 μ_B/f. u. at 9 T. The metamagnetic anomaly only along the a axis is in contrast with the successive metamagnetic anomalies along the c axis in the AFM ordered state of the quasikagome Ising system CePdAl [15]. Metamagnetic crossovers along the easy axis are often observed in paramagnetic states of Ce-based heavy fermion systems such as $CeRu_2Si_2$ [36]. The metamagnetic crossover is accompanied by the field-induced deformation of the Fermi surface [37].

The temperature dependence of the metamagnetic anomaly has been further studied by the measurements of isothermal ac susceptibility as a function of magnetic field. Figure 5(b) shows the results of $\chi_{ac}(B \parallel a)$ at several constant temperatures from 5 K to 0.03 K. Thereby, a broad hump at 5 T transforms to a peak at 5.5 T, whose value agrees with that of the peak in the field dependence of C/T in Fig. 5(c). To the best of our knowledge, no theoretical calculation has been reported for the magnetization process of spin-1/2 Ising kagome lattice even for insulating systems. This is in contrast with the case of the well-studied spin-1/2 Heisenberg kagome lattice where a magnetization plateau appears at 1/3 of the saturation moment [38]. Our observation of the metamagnetic crossover for $B \perp c$ requests theoretical investigation of the magnetization process of the Ising kagome lattice.

It is expected that the metamagnetic crossover in CeIrSn affects scattering of conduction electrons. Bearing this in mind, we have measured the magnetoresistance (MR) at various constant temperatures in the longitudinal ($B \parallel I$) and transverse ($B \perp I$) configurations. Figure 6 shows the sets of data of MR $= (\rho - \rho_0)/\rho_0$ normalized by the zero-field value ρ_0 as a function of external field B up to 17.5 T. At the lowest temperature 0.03 K, MR($B \parallel I \parallel a$) exhibits a sharp negative peak at 6.5 T. Before approaching the peak, the slope becomes largest at around 5.5 T, which agrees with the metamagnetic field in χ_{ac} and C/T. With increasing temperature, the field at the minimum in MR shifts to higher fields. A similar trend for the minimum of MR is observed in the configuration $B \parallel a$ and $I \parallel c$. A negative peak in MR($B \parallel c$, $I \parallel a$) appears at 0.4 T, which coincides with the field where the slope of $M(B \parallel c)$ markedly decreases [see Fig. 5(a)]. Interestingly, the positive contribution to the MR($B \parallel c$, $I \parallel a$) is in proportion to B up to 17.5 T. For CeRhSn, a linear MR($B \parallel c$ and $I \parallel a$) was also observed but remains unexplained [20]. In any case, the good correspondence between the magnetization process and the field dependence of MR indicates that the anomalies in both properties are not caused by impurity spins but are intrinsic to the quasikagome Kondo lattice.

It is instructive to compare the MR associated with the metamagnetic crossover in CeIrSn with those reported for CeRhSn, CePdAl, and $CeRu_2Si_2$. For CeRhSn, no remarkable anomalies were observed in the MR at the metamagnetic crossover field $B \parallel a = 3.5$ T [20]. The MR in the AFM state of CePdAl exhibits a positive peak at the first metamagnetic field $B \parallel c = 3.1$ T [15]. In the paramagnetic $CeRu_2Si_2$, the metamagnetic anomaly at $B \parallel c = 8$ T causes a positive and sharp peak in the MR [35]. The negative peak in MR($B \parallel a$) for CeIrSn must have different origin from the critical

scattering related with the field-induced elongation of the Ising-type moments in CePdAl and $CeRu_2Si_2$.

IV. CONCLUSION

We have studied structural, transport, and magnetic properties of single-crystalline samples of CeIrSn, in which the Ce atoms form a quasikagome lattice. The single-crystal x-ray diffraction analysis confirmed the absence of superstructure causing a structural disorder. At high temperatures, the valence fluctuating nature manifests itself in the broad maximum in $S_a(T)$ and $S_c(T)$. The estimated T_K of 480 K for CeIrSn is twice higher than that of the isostrucural and isoelectronic compound CeRhSn. The Ising nature in the susceptibility, $\chi_c(T) \gg \chi_a(T)$, and highly anisotropic resistivity, $\rho_a(T) > \rho_c(T)$, are similar to those in CeRhSn. Both $\rho_a(T)$ and $\rho_c(T)$ exhibit no kinklike anomaly down to 0.04 K, indicating the absence of long-range magnetic order.

On cooling below 7 K, $\chi_c(T)$ and $\chi_a(T)$ exceed the values for CeRhSn and diverge as T^{-n} with $n = 0.8$ and 0.6, respectively. The increase in C/T at $T < 0.1$ K is dominated by the Schottky specific heat arising from Ir nuclear quadrupoles. The estimated electronic part C_{el}/T becomes comparable with that of CeRhSn at around 0.15 K. The metamagnetic crossover in $M(B \parallel a)$ takes place at 5.5 T, which coincides with the positive peak in C/T and the negative peak in the MR under $B \parallel a$. Because the metamagnetic crossover occurs in both CeIrSn and CeRhSn under the field applied along the a axis, it seems to appear by the alleviation of magnetic frustration in the quasikagome Kondo lattice.

ACKNOWLEDGMENTS

The single-crystal x-ray diffraction measurements, electron-probe microanalysis, and magnetic and transport measurements were performed at Cryogenics and Instrumental Analysis Division, N-BARD, Hiroshima University. Part of this work was supported by NIMS Joint Research Hub Program and the Visiting Researcher's Program of the Institute of Solid State Physics, the University of Tokyo. We thank the financial support from JSPS KAKENHI Grants No. JP26400363, No. JP16H01076, and No. JP17K05545.

[1] M. Vojta, Rep. Prog. Phys. **81**, 064501 (2018).
[2] K. Barros, J. W. F. Venderbos, G.-W. Chern, and C. D. Batista, Phys. Rev. B **90**, 245119 (2014).
[3] H. Ishizuka and Y. Motome, Phys. Rev. B **91**, 085110 (2015).
[4] S. Ghosh, P. O'Brien, C. L. Henley, and M. Lawler, Phys. Rev. B **93**, 024401 (2016).
[5] A. Dönni, G. Ehlers, H. Maletta, P. Fischer, H. Kitazawa, and M. Zolliker, J. Phys.: Condens. Matter **8**, 11213 (1996).
[6] K. Umeo, K. Yamane, Y. Muro, K. Katoh, Y. Niide, A. Ochiai, T. Morie, T. Sakakibara, and T. Takabatake, J. Phys. Soc. Jpn. **73**, 537 (2004).
[7] G. M. Schmiedeshoff, E. D. Mun, A. W. Lounsbury, S. J. Tracy, E. C. Palm, S. T. Hannahs, J.-H. Park, T. P. Murphy, S. L. Bud'ko, and P. C. Canfield, Phys. Rev. B **83**, 180408(R) (2011).
[8] M. S. Kim and M. C. Aronson, Phys. Rev. Lett. **110**, 017201 (2013).
[9] M. Vojta, Phys. Rev. B **78**, 125109 (2008).
[10] P. Coleman and A. H. Nevidomskyy, J. Low Temp. Phys. **161**, 182 (2010).
[11] Q. Si, J. H. Pixley, E. Nica, S. J. Yamamoto, P. Goswami, R. Yu, and S. Kirchner, J. Phys. Soc. Jpn. **83**, 061005 (2014).
[12] *Introduction to Frustrated Magnetism: Materials, Experiments, Theory*, edited by C. Lacroix, P. Mendeles, and F. Mika (Springer, New York, 2011).
[13] F. Hulliger, J. Alloys Compd. **196**, 225 (1993).
[14] A. Oyamada, S. Maegawa, M. Nishiyama, H. Kitazawa, and Y. Isikawa, Phys. Rev. B **77**, 064432 (2008).
[15] T. Goto, S. Hane, K. Umeo, T. Takabatake, and Y. Isikawa, J. Phys. Chem. Solids **63**, 1159 (2002).
[16] A. Ślebarski, M. B. Maple, E. J. Freeman, C. Sirvent, M. Radłowska, A. Jezuerski, E. Granado, Q. Huang, and J. W. Lynn, Philos. Mag. B **82**, 943 (2002).
[17] M. S. Kim, Y. Echizen, K. Umeo, S. Kobayashi, M. Sera, P. S. Salamakha, O. L. Sologub, T. Takabatake, X. Chen, T. Tayama, T. Sakakibara, M. H. Jung, and M. B. Maple, Phys. Rev. B **68**, 054416 (2003).
[18] A. Schenck, F. N. Gygax, M. S. Kim, and T. Takabatake, J. Phys. Soc. Jpn. **73**, 3099 (2004).
[19] Y. Tokiwa, C. Stingl, M. S. Kim, T. Takabatake, and P. Gegenwart, Sci. Adv. **1**, e1500001 (2015).
[20] C. L. Yang, S. Tsuda, K. Umeo, Y. Yamane, T. Onimaru, T. Takabatake, N. Kikugawa, T. Terashima, and S. Uji, Phys. Rev. B **96**, 045139 (2017).
[21] R. Küchler, C. Stingl, Y. Tokiwa, M. S. Kim, T. Takabatake, and P. Gegenwart, Phys. Rev. B **96**, 241110(R) (2017).
[22] P. Salamakha, O. Sologub, J. K. Yakinhos, and Ch. D. Routsi, J. Alloys Compd. **265**, L1 (1998).
[23] B. Chevalier, C. P. Sebastian, and R. Pöttgen, Solid State Sciences **8**, 1000 (2006).
[24] M. F. Zumdick and R. Pöttgen, Z. Kristallogr. **214**, 90 (1999).
[25] Y. Echizen, K. Yamane, and T. Takabatake, Physica B **329-333**, 522 (2003).
[26] Y. Bando, T. Suemitsu, K. Takagi, H. Tokushima, Y. Echizen, K. Katoh, K. Umeo, Y. Maeda, and T. Takabatake, J. Alloys Compd. **313**, 1 (2000).
[27] M. D. Koterlyn, O. I. Babych, andG. M. Koterlyn, J. Alloys Compd. **325**, 6 (2001).
[28] Bruker (2016), *APEX3*, *SADABS*, and *SAINT*, Bruker AXS Inc., Madison, Wisconsin, USA.
[29] G. M. Sheldrick, Acta Cryst. A **71**, 3 (2015).
[30] E. Mun, S. L. Bud'ko, M. S. Torikachvili, and P. C. Canfield, Meas. Sci. Technol. **21**, 055104 (2010).
[31] H. Tsujii, B. Andraka, K. A. Muttalib, and Y. Takano, Physica B **329-333**, 1552 (2003).
[32] M. S. Kim, T. Sasakawa, Y. Echizen, and T. Takabatake, Jpn. J. Appl. Phys. **42**, 6512 (2003).

[33] D. T. Adroja, A. D. Hillier, S. Tsuda, C. Yang, and T. Takabatake (unpublished).
[34] D. Gignoux and J. C. Gomez-Sal, Phys. Rev. B **30**, 3967 (1984).
[35] A. Tari, *The Specific Heat of Matter at Low Temperatures* (Imperial College Press, London, 2003), p. 262.
[36] P. Haen, J. Flouquet, F. Lapierre, P. Lejay, and G. Remenyi, J. Low Temp. Phys. **67**, 391 (1987).
[37] H. Aoki, N. Kimura, and T. Terashima, J. Phys. Soc. Jpn. **83**, 072001 (2014).
[38] H. Nakano and T. Sakai, J. Phys. Soc. Jpn. **87**, 063706 (2018).